

VARIABLE STARS IN LARGE MAGELLANIC CLOUD GLOBULAR CLUSTERS II: NGC 1786*

CHARLES A. KUEHN^{1,2}, HORACE A. SMITH¹, MÁRCIO CATELAN^{3,4}, BARTON J. PRITZL⁵, NATHAN DE LEE^{1,6}, JURA BORISSOVA⁷

Draft version August 22, 2018

ABSTRACT

This is the second in a series of papers studying the variable stars in Large Magellanic Cloud globular clusters. The primary goal of this series is to study how RR Lyrae stars in Oosterhoff-intermediate systems compare to their counterparts in Oosterhoff I/II systems. In this paper, we present the results of our new time-series BV photometric study of the globular cluster NGC 1786. A total of 65 variable stars were identified in our field of view. These variables include 53 RR Lyraes (27 RRab, 18 RRC, and 8 RRd), 3 classical Cepheids, 1 Type II Cepheid, 1 Anomalous Cepheid, 2 eclipsing binaries, 3 Delta Scuti/SX Phoenicis variables, and 2 variables of undetermined type. Photometric parameters for these variables are presented. We present physical properties for some of the RR Lyrae stars, derived from Fourier analysis of their light curves. We discuss several different indicators of Oosterhoff type which indicate that the Oosterhoff classification of NGC 1786 is not as clear cut as what is seen in most globular clusters.

Subject headings: galaxies: Magellanic Clouds - stars: horizontal-branch - stars: variables: general - stars: variables: RR Lyrae

1. INTRODUCTION

This is the second in a series of papers focusing on the variable stars in globular clusters in the Large Magellanic Cloud (LMC). The goal of this series is to better understand the Oosterhoff dichotomy, the tendency for Milky Way globular clusters to be classified as either Oosterhoff I (Oo-I) or Oosterhoff II (Oo-II) objects, and how the Oosterhoff intermediate clusters in the nearby dwarf galaxies fit into that picture. The Oosterhoff groups are traditionally defined based on the average periods of the RRab stars with Oo-I clusters having an average RRab period of $\langle P_{ab} \rangle < 0.58$ days and Oo-II clusters having $\langle P_{ab} \rangle > 0.62$ days. In general Oo-II clusters also tend to be more metal-poor and have a larger ratio of first overtone to fundamental mode RR Lyrae. The period range between the two groups, $0.58 \leq \langle P_{ab} \rangle \leq 0.62$ days, is referred to as the Oosterhoff gap and is essentially unoccupied by Milky Way globular clusters. The

nearby dwarf galaxies and their globular clusters present a sharp contrast to this behavior as these extra-galactic clusters not only fall in the Oo-I and Oo-II groups, they also fall into the gap between these groups; in fact the extra-galactic objects seem to preferentially be located in the gap. These Oosterhoff-intermediate objects, as objects that fall in the gap are called, present a challenge for models that propose that the Milky Way halo was formed through the accretion of objects similar to the present day nearby dwarf galaxies as we would expect to see similar Oosterhoff properties in both samples if that were the case (Catelan 2009). The present understanding of the Oosterhoff phenomenon will be discussed in more detail in a future paper in this series. The first paper in this series, Kuehn et al. (2011), discussed the variable stars in the LMC globular cluster NGC 1466. In this paper we identify, classify, and discuss the variable stars found in the LMC globular cluster NGC 1786.

NGC 1786 is an old globular cluster that is located near the center of the LMC. Mucciarelli et al. (2009) found a metallicity of $[Fe/H] = -1.75 \pm 0.01$ from high-resolution spectroscopy of seven red giant stars. However, Olszewski et al. (1991) found a slightly lower value of -1.87 ± 0.20 from the low-resolution spectra of two giant stars; these values are consistent within the error bars. Sharma et al. (2010) reported that NGC 1786 is not very reddened, having an $E(B-V) = 0.06$, and has an age of 12.3 Gyr. This age is consistent with Johnson et al. (2002) finding, through the comparison of the cluster color-magnitude diagram (CMD) with theoretical isochrones, that NGC 1786 formed within 2 Gyr of the other old LMC clusters.

NGC 1786 is a fairly centrally concentrated cluster which, combined with its location near the center of the LMC, makes it difficult to get accurate photometry of the stars in the center due to blending. Graham (1985) was the first to detect variable stars in NGC 1786, finding 12 variables, for which he determined periods of 10.

* Based on observations taken with the SMARTS 1.3-meter telescope operated by the SMARTS Consortium and observations taken at the Southern Astrophysical Research (SOAR) telescope, which is a joint project of the Ministério da Ciência, Tecnologia, e Inovação (MCTI) da República Federativa do Brasil, the U.S. National Optical Astronomy Observatory (NOAO), the University of North Carolina at Chapel Hill (UNC), and Michigan State University (MSU).

¹ Department of Physics and Astronomy, Michigan State University, East Lansing, MI 48824, USA; smith@pa.msu.edu

² Current address: Sydney Institute for Astronomy, University of Sydney, Sydney, Australia; kuehn@physics.usyd.edu.au

³ Pontificia Universidad Católica de Chile, Facultad de Física, Departamento de Astronomía y Astrofísica, Santiago, Chile; mcatelan@astro.puc.cl

⁴ The Milky Way Millennium Nucleus, Santiago, Chile

⁵ Department of Physics and Astronomy, University of Wisconsin Oshkosh, Oshkosh, WI 54901, USA; pritzlb@uwosh.edu

⁶ Current address: Department of Physics and Astronomy, Vanderbilt University, Nashville, TN 37235, USA; nathan.delee@vanderbilt.edu

⁷ Departamento de Física y Astronomía, Facultad de Ciencias, Universidad de Valparaíso, Valparaíso, Chile; jura.borissova@uv.cl

Walker & Mack (1988) later observed NGC 1786 and confirmed the variable nature of 11 of Graham’s stars, though they were also only able to determine periods for ten of the stars. Of the variables with known periods, 4 were classified as RRab stars, 5 as RRC stars, and one as a likely Anomalous Cepheid (AC).

More recently the Optical Gravitational Lensing Experiment-III (OGLE-III) observed the central portion of the LMC and many of its associated globular clusters, including NGC 1786 (Udalski et al. 2008). The OGLE-III survey is designed to find instances of gravitational lensing, but a natural consequence of this project is the discovery and monitoring of variable stars. OGLE-III greatly increased the number of identified variable stars in NGC 1786. A total of 55 RR Lyrae stars within 2 arcminutes of the cluster center were reported by Soszyński et al. (2009): 28 RRab, 18 RRC, and 9 RRd stars. The location of NGC 1786 near the center of the LMC means that some of these RR Lyrae stars likely belong to the field population of the LMC and not to the cluster.

In this paper we present the results of a new, ground-based search for variable stars in NGC 1786. We use the RR Lyrae in the cluster to determine the distance modulus and Oosterhoff classification of the cluster. We also present physical properties for the RR Lyrae stars determined through Fourier fitting of their light curves.

2. OBSERVATIONS AND DATA ANALYSIS

A total of 57 V and 56 B images were obtained using the SOI imager (5.2x5.2 arcminute field of view) on the SOAR 4-m telescope in November of 2007 and February of 2008 while 43 V and 42 B images were obtained using ANDICAM (6x6 arcminute field of view) on the SMARTS 1.3-m telescope operated by the SMARTS consortium⁸ from September 2006 to January 2007. SOAR exposure times were between 30s and 600s for V and between 60s and 900s for B . SMARTS exposure times were 450s in each filter. Table 1 lists the UT dates and times and time of each observation, which telescope it was on, the filter, and the seeing.

Data reduction and variable identification were carried out in the manner described in the first paper in the series, Kuehn et al. (2011). Photometry was converted to the standard system using standard stars from Stetson (2000) which were located within the field of NGC 1786. Of the 25 Stetson standard stars that appeared in our observations, the average difference between our photometry and that of Stetson is 0.002 ± 0.008 mags in V and 0.002 ± 0.011 mags in B . The majority of the identified variable stars were found in both the SOAR and SMARTS data however there was some disagreement between the two data sets existed for some of the more crowded stars. In the cases where there was disagreement we used the SOAR results due to its better resolution. The extremely crowded nature of NGC 1786 meant that the image subtraction package ISIS (Alard 2000) had to be used extensively to locate variable stars in the center of the cluster. As stated in Kuehn et al. (2011), periods of the variable stars are typically good to ± 0.0001 or 0.0002 days. Aliasing with the RRd stars limits derived period ratios to an accuracy of 0.001.

⁸ www.astro.yale.edu/smarts

3. VARIABLE STARS

A total of 65 variable stars were found within the SOAR 5.2×5.2 arcminute² field of view in the direction of NGC 1786. This includes the cluster as well as the surrounding area. The variables include 53 RR Lyraes (27 RRab, 18 RRC, and 8 RRd), 3 classical Cepheids, 1 Type II Cepheid, 1 Anomalous Cepheid, 2 eclipsing binaries, 3 Delta Scuti/SX Phoenicis variables, and 2 variables of undetermined type. The extreme crowding in the central region of NGC 1786 posed some difficulties for the identification and classification of the variable stars due to many of the stars being blended with near neighbors. Table 2 lists the identified variables, with the exception of the RRd stars which are listed in Table 3, their classification, period V and B amplitudes, intensity-weighted mean magnitudes, and magnitude-weighted mean $B - V$ color. Variable stars V01 through V11 were originally found by Graham (1985) and have periods confirmed by Walker & Mack (1988). The names for these stars are the same as the ones used by Graham and Walker & Mack. The positions of the variable stars are shown in Figures 1 and 2.

3.1. Field Contamination

NGC 1786’s location toward the center of the LMC means that a significant amount of contamination from LMC field stars is expected in the images. This makes it difficult to determine with absolute certainty whether an individual variable star is a member of the cluster. NGC 1786 has a tidal radius of 2.9 arcminutes (McLaughlin & van der Marel 2005), and 61 of the 65 variable stars are located within that tidal radius; the tidal radius does extend beyond the western edge of our field, and slightly beyond the northern and southern edges. The 4 stars (1 RRab, 1 RRC, 1 classical Cepheid, and 1 Delta Scuti/SX Phoenicis) outside the tidal radius are not cluster members and they are noted in Table 2 with the word “Field” after their name. The field of view in the images obtained with SOAR is 5.2×5.2 arcminutes² and a visual inspection shows that roughly 75% of the image is contained within the tidal radius of NGC 1786. The LMC field should feature a roughly even distribution of variable stars, thus the majority of the 61 variables found within the tidal radius should be members of the cluster. Classical Cepheids are younger stars, thus the two classical Cepheids that are within the tidal radius of NGC 1786 should be members of the LMC field. The amount of LMC field star contamination is still significant within the tidal radius of the cluster, as can be seen in Figures 3 and 4, where the presence of the field stars makes it difficult to distinguish a horizontal branch in the CMD for NGC 1786. The scatter in the position of the RR Lyrae stars in the CMD is likely due to the crowded nature of the central region of the cluster, which results in many of the RR Lyrae being partially blended with nearby stars, affecting their brightness and color.

The OGLE-III database (Soszyński et al. 2009) can also be used to get a better understanding of the amount of LMC field star contamination within the tidal radius of NGC 1786. We looked at an annulus centered on NGC 1786 which had the same area on the sky as contained within the tidal radius of the cluster, but which had a radius greater than the tidal radius. Within that annu-

Table 1
Observing Log

DATE (UT)	TIME (UT)	FILTER	Exp Time (s)	Seeing (arcseconds)	Telescope
2006-12-16	01:38:35	B	450.0	2.16	SMARTS
2006-12-16	01:47:03	V	450.0	1.83	SMARTS
2006-12-22	01:24:48	B	450.0	1.54	SMARTS
2006-12-22	01:33:16	V	450.0	1.12	SMARTS
2006-11-18	02:51:41	B	450.0	2.01	SMARTS

Note. — This table is published in its entirety in the electronic edition.

Table 2
Photometric Parameters for Variables in NGC 1786, Excluding RRd Stars

ID	RA (J2000)	DEC (J2000)	Type	P (days)	A_V	A_B	$\langle V \rangle$	$\langle B \rangle$	$\langle B - V \rangle$	OGLE-III ID
V01	04:58:51.3	-67:44:23.7	AC	0.80006	0.61	0.71	17.774	18.133	0.367	ACEP-009
V03	04:59:00.4	-67:44:40.3	RRab	0.62198	0.83	1.17	19.448	19.956	0.528	RRLYR-02661
V04	04:59:01.1	-67:43:29.4	RRab	0.55585	1.13	1.36	19.202	19.559	0.391	RRLYR-02662
V05	04:59:02.8	-67:46:06.0	RRab	0.69706	0.59	0.80	19.301	19.726	0.439	RRLYR-02674
V06	04:59:07.9	-67:45:29.4	RRc	0.30418	0.60	0.71	19.449	19.760	0.312	RRLYR-02712
V07	04:59:08.9	-67:44:08.0	RRc	0.29536	0.56	0.75	19.292	19.603	0.325	RRLYR-02727
V08	04:59:12.0	-67:43:52.6	RRab	0.57183	0.91	1.17	19.227	19.661	0.456	RRLYR-02748
V09	04:59:12.5	-67:44:15.0	RRc	0.36388	0.47	0.56	19.445	19.571	0.132	RRLYR-02757
V10	04:59:14.1	-67:44:23.7	RRab	0.69651	0.69	0.79	19.474	19.950	0.480	RRLYR-02770
V11	04:59:14.8	-67:44:21.3	RRc	0.31536	0.54	0.63	19.339	19.608	0.275	RRLYR-02777
V13	04:59:08.9	-67:44:39.6	RRab	0.55944	0.36	0.68	17.761	18.500	0.746	-
V14	04:59:03.1	-67:44:39.1	RRc	0.31786	0.62	0.77	19.473	19.806	0.345	RRLYR-02676
V15	04:59:09.4	-67:44:39.0	RRab	0.74962	0.35	-	18.26	-	-	RRLYR-02732
V17	04:59:06.3	-67:44:38.3	RRab	0.52470	0.33	0.68	17.855	18.693	0.852	RRLYR-02697
V18	04:59:11.4	-67:44:36.3	RRab	0.64515	0.97	1.20	19.083	19.491	0.439	RRLYR-02747
V19	04:59:04.2	-67:44:35.6	RRab	0.74479	0.43	0.57	18.807	19.322	0.522	RRLYR-02680
V20	04:59:09.4	-67:44:34.4	?	0.29193	-	0.43	-	19.215	-	-
V22	04:59:10.1	-67:44:27.2	RRc	0.32920	0.63	0.72	19.330	19.564	0.243	RRLYR-02738
V23	04:59:04.8	-67:44:24.9	RRab	0.52851	0.50	0.93	18.383	19.030	0.672	RRLYR-02683
V24	04:59:11.2	-67:44:17.4	RRc	0.41110	0.30	0.39	18.682	18.955	0.275	RRLYR-02743/02746
V25-Field	04:59:41.3	-67:44:16.8	Ceph	3.27005	0.84	1.16	15.694	16.258	0.601	CEP-0591
V26	04:59:09.2	-67:44:14.3	RRab	0.73891	0.39	0.48	19.179	19.630	0.455	RRLYR-02729
V27	04:59:14.5	-67:43:52.2	RRab	0.66428	0.58	0.60	18.990	19.234	0.245	RRLYR-02776
V30	04:59:07.2	-67:43:30.9	Ceph	11.6769	0.93	1.55	14.236	14.799	0.607	CEP-0561
V31	04:59:06.6	-67:43:26.2	Eclipse	0.61/1.2	-	-	18.340	18.376	0.036	-
V32-Field	04:59:34.7	-67:42:46.7	RRab	0.532071	1.11	1.46	19.089	19.373	0.325	RRLYR-02855
V33 BL	04:59:28.9	-67:42:40.1	RRab	0.53278	0.67	0.71	19.587	20.028	0.430	RRLYR-02834
V34	04:58:59.3	-67:42:38.3	Eclipse	1.6/3.2	-	-	19.514	19.754	0.240	-
V35-Field	04:59:36.0	-67:42:31.9	RRc	0.33058	0.48	0.57	19.190	19.556	0.371	RRLYR-02864
V36-Field	04:59:39.4	-67:42:15.1	Delta Scuti	0.07723	0.56	0.62	20.319	20.485	0.172	DSCT-400
V37	04:59:09.0	-67:46:14.9	RRc	0.35488	0.44	0.57	19.353	19.584	0.239	RRLYR-02728
V38	04:59:21.2	-67:46:06.7	RRab	0.75890	0.40	0.47	19.014	19.438	0.427	RRLYR-02802
V39	04:59:03.0	-67:45:36.2	Delta Scuti	0.08040	0.28	0.41	20.699	21.044	0.349	-
V40	04:58:59.6	-67:45:24.6	RRc	0.33496	0.55	0.66	19.631	20.026	0.403	RRLYR-02657
V41	04:59:06.1	-67:45:24.4	T2Ceph	1.108051	0.86	1.07	18.488	18.928	0.461	T2CEP-020
V42	04:59:01.4	-67:45:21.5	RRc	0.37064	0.45	0.58	19.307	19.624	0.325	RRLYR-02667
V43	04:58:49.9	-67:45:10.7	Delta Scuti	0.06096	0.70	0.84	21.365	21.636	0.283	-
V44	04:59:15.6	-67:45:02.9	RRc	0.36459	0.51	0.58	19.294	19.640	0.348	RRLYR-02781
V45	04:59:08.8	-67:45:01.9	RRc	0.29913	0.68	0.71	19.389	19.560	0.180	RRLYR-02724
V46	04:59:09.2	-67:45:01.6	Ceph	2.16488	0.30	0.41	15.817	16.491	0.679	CEP-0563
V49	04:59:05.7	-67:44:55.9	?	0.55403	0.20	0.24	17.294	18.223	0.929	-
V50	04:59:10.0	-67:44:55.6	RRab	0.49336	0.74	0.88	18.601	18.866	0.263	RRLYR-02737
V51	04:59:03.0	-67:44:54.1	RRab	0.56363	0.40	0.58	18.335	18.898	0.574	RRLYR-02675
V52	04:59:09.3	-67:44:53.4	RRc	0.32653	0.47	0.57	18.989	19.317	0.333	RRLYR-02730
V54	04:59:05.0	-67:44:51.8	RRc	0.30898	0.41	0.48	19.332	19.669	0.339	RRLYR-02686
V55 BL	04:59:08.9	-67:44:51.7	RRab	0.51904	0.97	1.14	18.720	18.860	0.154	RRLYR-02725
V56	04:59:04.0	-67:44:50.7	RRab	0.52757	0.44	0.67	19.736	20.036	0.318	RRLYR-02678
V57	04:59:09.5	-67:44:50.5	RRab	0.52083	-	-	-	-	-	RRLYR-02733
V58	04:59:04.9	-67:44:49.1	RRab	0.55049	0.63	0.712	18.821	19.185	0.371	RRLYR-02685
V59	04:59:07.3	-67:44:48.7	RRab	0.56507	-	-	-	-	-	RRLYR-02706
V60	04:59:11.6	-67:44:46.8	RRc	0.29205	0.32	0.42	19.217	19.502	0.289	-
V61	04:59:12.0	-67:44:43.9	RRc	0.36061	0.44	0.60	19.302	19.896	0.597	RRLYR-02749
V62	04:59:05.9	-67:44:43.3	RRc	0.36411	0.28	0.44	18.969	19.512	0.550	RRLYR-02692
V63	04:59:07.9	-67:44:48.6	RRab	0.62312	-	-	-	-	-	RRLYR-02714
V64	04:59:07.8	-67:44:52.6	RRab	0.70228	-	-	-	-	-	RRLYR-02711
V65	04:59:06.6	-67:44:42.0	RRab	0.64660	-	-	-	-	-	RRLYR-02702
V66	04:59:07.5	-67:44:35.7	RRab	0.50999	-	-	-	-	-	RRLYR-02671

Table 3
Photometric Parameters for the RRd Variables in NGC 1786

ID	RA	DEC	Type	P_0 (days)	P_1 (days)	P_1/P_0	$A_{V,0}$	$A_{V,1}$	$A_{B,0}$	$A_{B,1}$	$\langle V \rangle$	$\langle B \rangle$	$\langle B - V \rangle$	OGLE-III ID
V02	04:58:52.6	-67:43:53.8	RRd	0.4876	0.3630	0.7445	0.24	0.38	0.20	0.50	19.144	19.442	0.306	RRLYR-02626
V16	04:59:06.0	-67:44:39.6	RRd	0.4838	0.3601	0.7443	-	-	-	-	-	-	-	RRLYR-02693
V21	04:58:59.3	-67:44:32.1	RRd	0.4937	0.3676	0.7447	0.16	0.46	0.22	0.58	19.443	19.806	0.367	RRLYR-02653
V28	04:58:59.7	-67:43:52.1	RRd	0.4876	0.3631	0.7447	0.28	0.44	0.32	0.62	19.200	19.493	0.308	RRLYR-02658
V29	04:59:14.1	-67:43:46.2	RRd	0.4955	0.3694	0.7455	-	0.26	-	0.38	19.083	19.523	0.444	RRLYR-02771
V47	04:59:06.2	-67:44:56.3	RRd	0.4969	0.3699	0.7444	-	0.75	-	1.00	19.977	20.444	0.491	RRLYR-02698
V48	04:59:12.2	-67:44:56.3	RRd	0.4801	0.3574	0.7445	0.28	0.36	0.46	0.36	19.324	19.729	0.409	RRLYR-02750
V53	04:59:05.6	-67:44:52.8	RRd	0.4918	0.3661	0.7444	-	-	-	-	-	-	-	RRLYR-02688

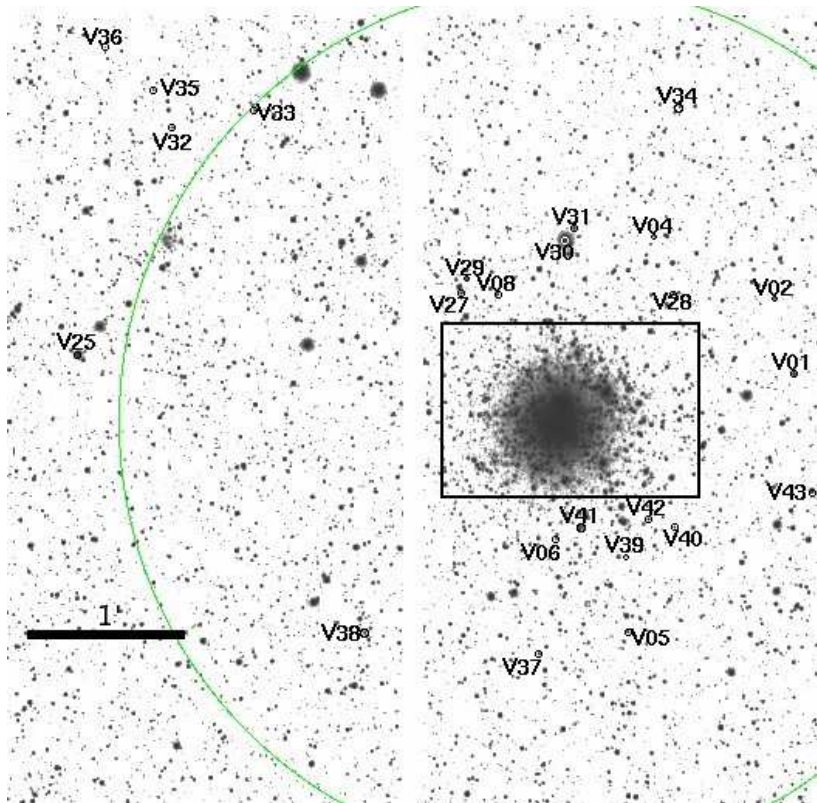


Figure 1. Finding chart for the variable stars in the outer portion of NGC 1786. North is up and East is to the left. The white gap is due to the finding chart being made from a SOAR image and represents the 7.8 arcsec mounting gap between the two CCDs of the SOI camera. The large green circle shows the tidal radius of the cluster while the black box shows the region that is shown in Figure 2.

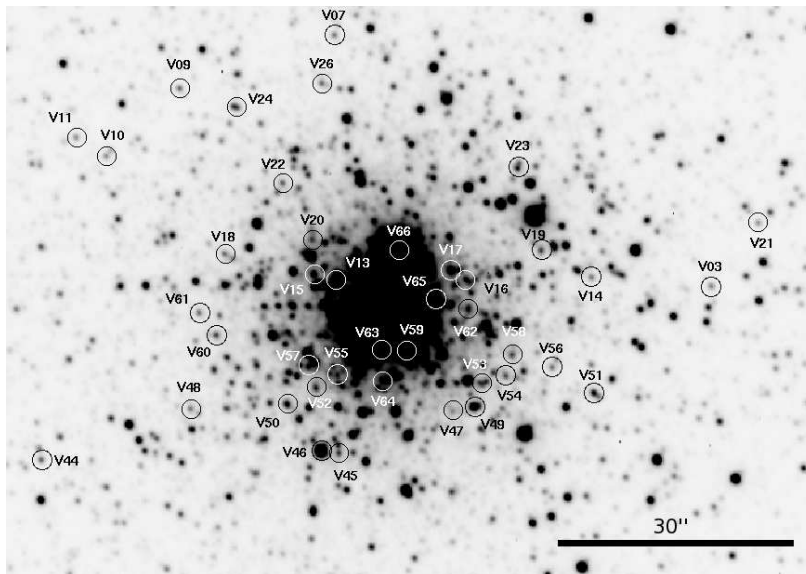


Figure 2. Finding chart for the variable stars in the inner portion of NGC 1786. North is up and East is to the left.

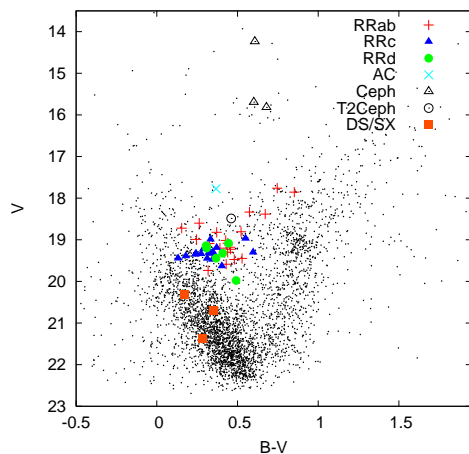


Figure 3. $V, B-V$ CMD for stars within the tidal radius of NGC 1786 with the positions of the RR Lyrae variables also indicated. Plus symbols indicate RRab stars, filled triangles indicate RRc's, and circles indicate RRd's. The contamination by LMC field stars is readily apparent. The scatter in the positions of the RR Lyrae stars is a consequence of blending that arises from the crowded nature of the central region of the cluster.

lus OGLE-III found 7 RRab, 2 RRc, 1 classical Cepheid, and 1 Delta Scuti star. Within the 2.9 arcminute tidal radius OGLE-III found 31 RRab, 19 RRc, 9 RRd, 1 Type II Cepheid, 2 classical Cepheids, 1 Anomalous Cepheid. As previously mentioned, the classical Cepheids cannot be cluster members due to their ages and the numbers of Type II and Anomalous Cepheids are too small to be able to say anything about the likelihood of their membership in the cluster in a statistical way. Since there is no reason to suspect a significant variation in the distribution of LMC field RR Lyrae stars over the size of the fields in question, it is reasonable to suspect that approximately 15% of the RR Lyrae stars found within the tidal radius of NGC 1786 to actually be members of the LMC field. It is interesting to note that the a large majority of the RR Lyrae stars found in the comparison field are RRab stars and none of them are RRd stars; this is a marked contrast to what is found within the tidal ra-

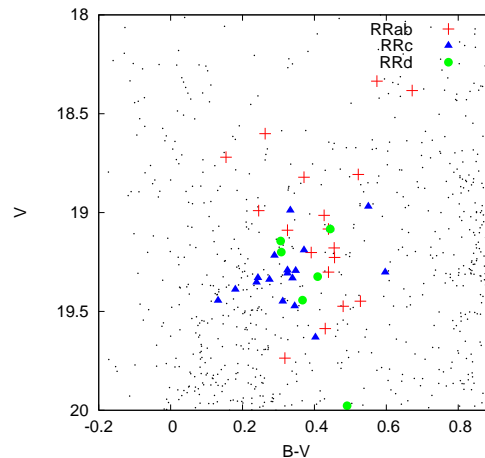


Figure 4. $V, B-V$ CMD for NGC 1786 that is zoomed in on the horizontal branch. The symbols used are the same as in Figure 3 where 32% of the RR Lyrae are RRc and 15% are RRd. Based on this we should expect that the majority of LMC field RR Lyrae within the tidal radius are RRab stars and that the ratio of first overtone dominant RR Lyrae to total number of RR Lyrae among cluster members is higher than suggested by the numbers found within the tidal radius; this will be discussed in more detail later in this paper when we discuss the Oosterhoff classification of NGC 1786.

3.2. RR Lyrae Stars

A total of 26 RRab, 17 RRc, and 8 RRd stars were found within the tidal radius of NGC 1786; 1 RRab and 1 RRc are new discoveries that have not been found in any of the previous studies of the cluster. All of the 9 RR Lyrae stars originally identified by Graham (1985) were found. V2 had been classified as an RRc star by Graham (1985) and Walker & Mack (1988). However, the larger number of epochs in our data set allowed for the detection of a second pulsation mode in this star, and it has accordingly been reclassified as an RRd star. For these nine stars originally found by Graham, we obtained intensity-weighted mean magnitudes of $\langle V \rangle = 19.321 \pm 0.039$

Table 4
Photometry of the Variable Stars

ID	Filter	HJD	Phase	Mag	Mag Error	Telescope
V01	<i>B</i>	2453981.8230	0.11033	17.878	0.013	SMARTS
V01	<i>B</i>	2453988.7630	0.78468	18.230	0.070	SMARTS
V01	<i>B</i>	2453991.7793	0.55477	18.703	0.063	SMARTS
V01	<i>B</i>	2453993.8316	0.11995	17.971	0.015	SMARTS
V01	<i>B</i>	2453995.8099	0.59264	18.564	0.021	SMARTS

Note. — Maximum light occurs at a phase of 0. This table is published in its entirety in the electronic edition.

and $\langle B \rangle = 19.677 \pm 0.059$. These are fainter than Walker & Mack’s values ($\langle V \rangle = 19.203 \pm 0.073$ and $\langle B \rangle = 19.526 \pm 0.066$). This disagreement in brightness is potentially due to the improved resolution of our observations, decreasing the effect of blending between the RR Lyrae stars and other nearby stars. V08 shows strong indications of being blended in Walker & Mack’s data, appearing brighter than the other RR Lyrae, while in our data it has a similar brightness to the other RR Lyrae. We also found large amplitudes for V08 in our data than were obtained by Walker & Macks ; this is expected for a blended star. If we remove V08 from the calculation, the mean magnitudes for the RR Lyrae from Walker & Mack become $\langle V \rangle = 19.271 \pm 0.030$ and $\langle B \rangle = 19.573 \pm 0.052$; these are much closer to the values we obtained. For the entire set of RR Lyrae stars within the tidal radius found in our study, the mean magnitudes are $\langle V \rangle = 19.241 \pm 0.047$ and $\langle V \rangle = 19.594 \pm 0.052$; these values are brighter than our values for just the stars that were originally found by Graham. Since the majority of the new RR Lyrae were found toward the crowded cluster center, one would expect that they would more likely suffer from blending and thus appear brighter, this is discussed in Section 5. Sample light curves for the RR Lyrae stars in NGC 1786 are shown in Figures 5-8 with the SOAR data shown indicated by crosses and the SMARTS data by points with a horizontal line; the full set of light curves can be found in the electronic version of this paper. Table 4 contains the photometric data for the variable stars.

Soszyński et al. (2009) found 57 RR Lyrae stars within the tidal radius of NGC 1786 using the OGLE-III data. We found 51 of these stars in our data; the remaining six are located within the extremely crowded core of the cluster. These six stars were only found in the OGLE *I*-band data, likely due to the seeing be better in *I* than in *B* or *V*.

Soszyński et al. (2009) found 9 RRd stars, all of which show up in our data but only 8 of which we classified as RRd stars. V16 (OGLE-III RRLYR-02693), V29 (OGLE-III RRLYR-02771), V47 (OGLE-III RRLYR-02698), and V53 (OGLE-III RRLYR-02688) were all classified as an RRd stars by Soszyński et al. (2009); however, while they do display some possible double-mode behavior, we were unable to determine second periods for these stars. While our data set is larger in the *V*-band than the OGLE-III data set, OGLE-III’s *I*-band has far more observation than either *V*-band data set and is thus better equipped for the determination of secondary periods in double-mode variables. Our data does not contradict OGLE-III’s results for these stars so we

have classified these four stars as RRd. The listed periods for these stars in Table 3 are taken from OGLE-III; the lack of listed amplitudes for the fundamental mode for these stars comes from our inability to find reliable second periods for them.

OGLE-III RR LYR-02746 was classified as an RRd star by Soszyński et al. (2009) but is only slightly seperated on the sky from OGLE-III RRLYR-02743 (≈ 0.15 arcseconds) and these can potentially be a single star. Our photometry only found one variable star at this location, V24, which has appears to be an RRc star, though the light curve is noisy. We were unable to find any secondary periods for this star and it is likely that the noisy light curve is a result of blending with nearby non-variable neighbors; this would also explain the star being brighter than the horizontal branch.

V48 (OGLE-III RRLYR-02750) is an RRd star however it is questionable if it is a first overtone dominant RRd star or a fundamental-mode dominant pulsator. The *V*-band light curve indicates the first overtone amplitude is larger, which agrees with the *I*-band results from Soszyński et al. (2009). However, the *B*-band data suggests that the fundamental-mode amplitude is larger. Since there are more *V*-band data points, we have decided to consider the first overtone dominant in V48 when it comes to determining the number ration of first overtone dominant pulsators to fundamental-mode pulsators. This agrees with the results from OGLE-III’s *I*-band data which indicated the first overtone was dominant.

V13, V15 (OGLE-III RRLYR-02732), V17 (OGLE-III RRLYR-02697), V23 (OGLE-III RRLYR-02683), and V15 (OGLE-III RRLYR-02675) are all RR Lyrae stars that are at least one magnitude brighter than the mean for the other RR Lyrae stars and have amplitudes that are smaller than expected for their period. These stars are all located toward the center of the cluster and are likely blended; the difference in amplitude is exactly what you would expect from the amount of blending needed to increase their magnitude to the observed level. Because of this blending we do not include these 5 stars when calculating the average brightnesses of the NGC 1786 RR Lyraes; they are included in all mean period determinations as blending has no impact on the observed period.

V33 (OGLE-III RRLYR-02834) features a light curve that suggests that it may exhibit the Blazhko effect. V55 (OGLE-III RRLYR-02725) also features a light curve that suggests a possible Blazhko effect but this star is a bit brighter than the other RR Lyrae stars and thus it is possible the noise in the light curve is a result of blending. These stars are indicated as being possible Blazhko

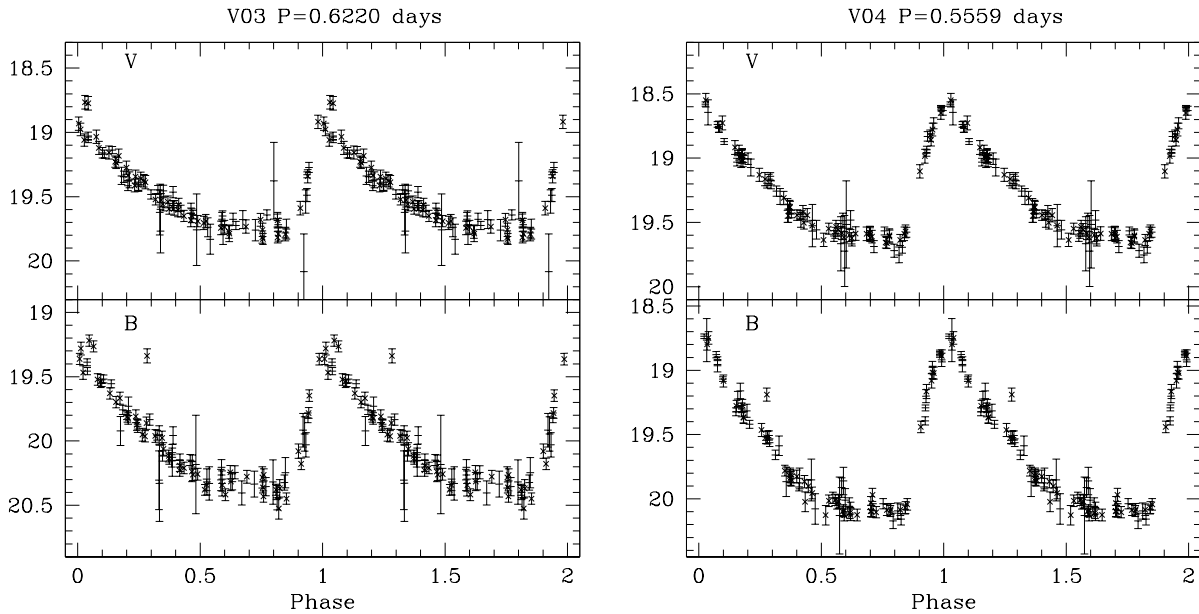


Figure 5. Sample light curves for RRAb stars in NGC 1786. SOAR data is indicated with crosses while SMARTS data is indicated by points with horizontal lines. (The full set of light curves can be found in the electronic version of this paper.)

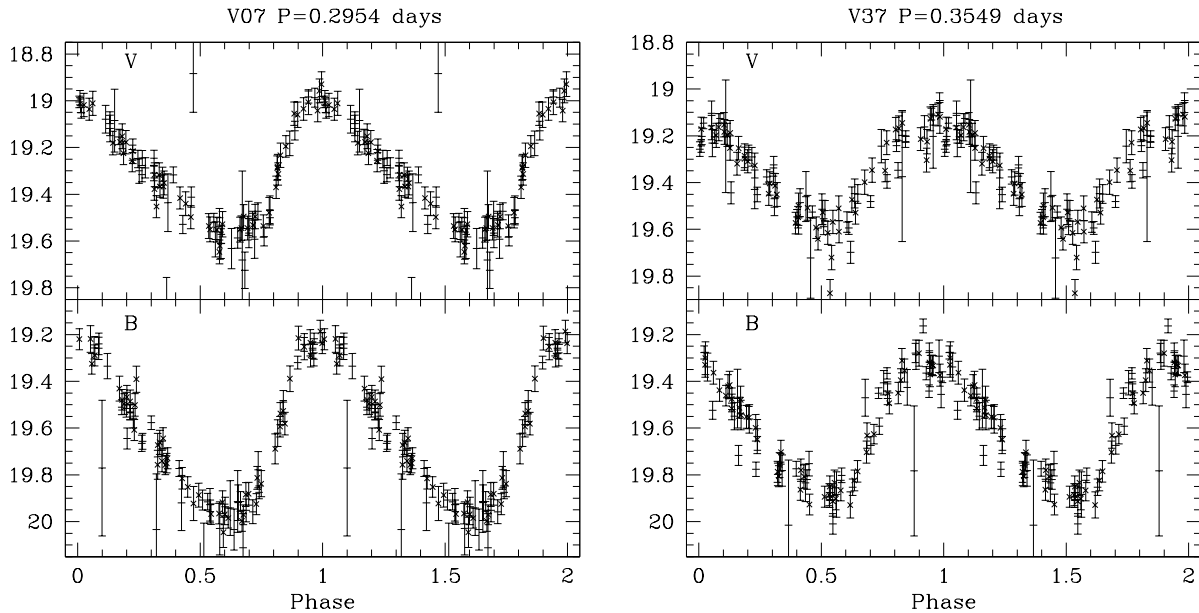


Figure 6. Sample light curves for RRc stars in NGC 1786. SOAR data is indicated with crosses while SMARTS data is indicated by points with horizontal lines. (The full set of light curves can be found in the electronic version of this paper.)

stars by the letters 'BL' in Table 2.

ISIS was used to find 9 of the RR Lyrae stars (V15, V16, V53, V57, V59, V63-V66); the location of these stars in the extremely crowded center of the cluster did not allow Daophot light curves to be obtained.

3.3. Other Variables

In addition to the RR Lyrae stars, our field of view contained 3 classical Cepheids, 1 Type II Cepheid, 1 Anomalous Cepheid, 2 eclipsing binaries, and 3 stars that are either Delta Scuti or SX Phoenicis variables. These classifications were determined based on the period, brightness,

and light curve shape; these classifications agree with those from OGLE-III and the literature.

V25, V30, and V46 are all classical Cepheids. As classical Cepheids are much younger stars than RR Lyrae's, they should be members of the LMC field population. The fact that two of the three classical Cepheids fall within the tidal radius of NGC 1786 on the image, is an indication that the LMC field population makes a significant contribution to the number of variable stars that fall in this region.

Three short period variables, V36, V39, and V43, were found and have been classified as either Delta Scuti

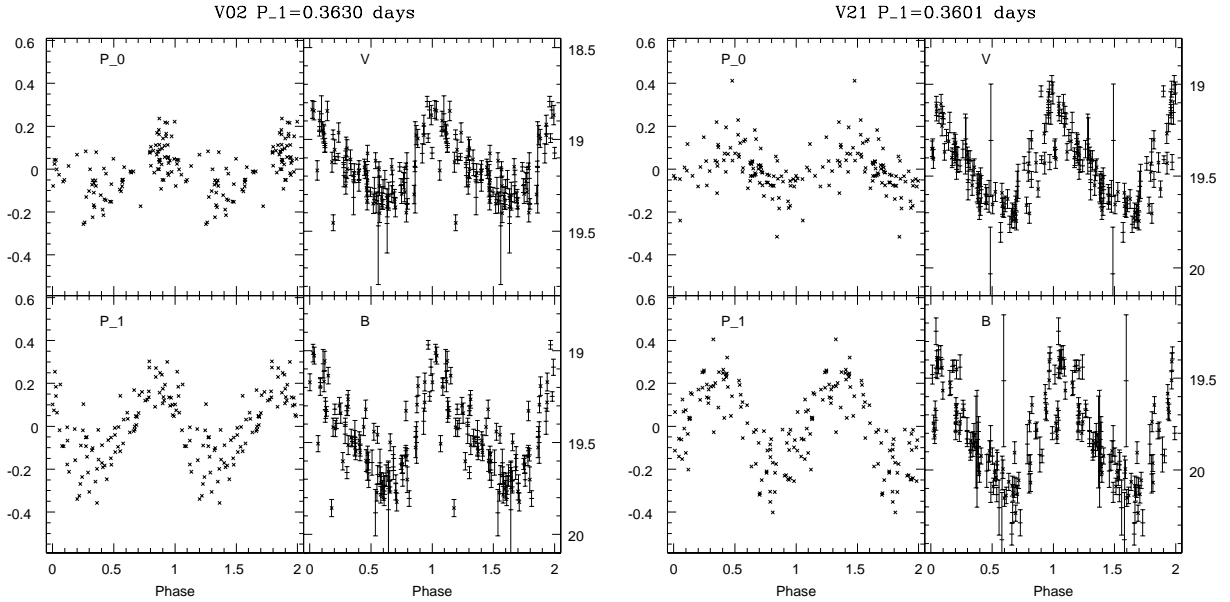


Figure 7. Sample light curves for RRd stars in NGC 1786. The left panels show the residuals left from subtracting the fundamental or first overtone periods. The right panels show the V and B -band light curves plotted with the first overtone period. SOAR data is indicated with crosses while SMARTS data is indicated by points with horizontal lines. (The full set of light curves can be found in the electronic version of this paper.)

Table 5
Fourier Coefficients for RRab Variables

ID	A_1	A_{21}	A_{31}	A_{41}	ϕ_{21}	ϕ_{31}	ϕ_{41}	D_{max}	Order
V03	0.369	0.446	0.249	0.178	2.47	5.03 ± 0.18	1.25	46.35	6
V04	0.454	0.396	0.232	0.090	2.30	4.93 ± 0.10	1.09	26.97	10
V05	0.229	0.397	0.318	0.122	2.26	5.54 ± 0.17	2.34	12.15	7
V08	0.308	0.492	0.320	0.107	2.13	4.75 ± 0.27	1.20	5.65	7
V10	0.235	0.564	0.300	0.173	2.39	4.97 ± 0.30	1.76	6.73	7
V26	0.175	0.377	0.153	0.076	2.46	5.88 ± 0.36	2.27	39.77	8
V38	0.161	0.336	0.192	0.102	2.96	6.05 ± 0.32	2.32	8.42	7

stars, which would be part of the LMC field, or SX Phoenicis stars, which would be member of NGC 1786. Soszyński et al. (2009) classified V36 (OGLE-III DSCT-400) as a Delta Scuti and its location outside of the tidal radius of NGC 1786, making it an LMC field star, is consistent with it most likely being a Delta Scuti.

Two eclipsing binaries, V31 and V34, were found. Potential periods are listed in Table 1 but we did not have enough observations to definitively determine periods.

4. PHYSICAL PROPERTIES OF THE RR LYRAE STARS

Physical properties for the RR Lyrae stars were determined using the Fourier decomposition method. The RRab light curves were fit with a Fourier series of the form

$$m(t) = A_0 + \sum_{j=1}^n A_j \sin(j\omega t + \phi_j), \quad (1)$$

while the RRc light curves were fit with a cosine series. The resulting Fourier coefficients were then used to calculate physical properties of the stars using the relations from Jurcsik & Kovács (1996), Jurcsik (1998), Kovács & Walker (1999, 2001), Simon & Clement (1993), and Morgan, Wahl, & Wieckhorst (2007). Full details of this

method are discussed in the first paper in this series (Kuehn et al. 2011).

We attempted to fit Fourier series to the light curves of all the RR Lyrae stars but only 7 RRab and 7 RRc stars had light curves of sufficient quality to allow for a successful fit. One of the RRc stars, V35, is located outside of the tidal radius of NGC 1786 and is thus a member of the LMC field, this is indicated in the tables. Tables 5 and 6 list the Fourier coefficients for the RRab and RRc stars, respectively, while Tables 7 and 8 list the physical properties of these stars. The averages of the physical properties for the RRc stars are calculated using only the 6 stars within the tidal radius of the cluster. Table 5 also lists the D_m value from Jurcsik & Kovács (1996). Lower D_m values indicate RRab stars with more “regular” light curves while higher values indicating those with more “anomalous” light curves.

The mean metallicity for the RRab stars is $[\text{Fe}/\text{H}]_{\text{J95}} = -1.48 \pm 0.14$ in the scale of Jurcsik (1995). This can be transformed into the Zinn & West (1984) scale using the relation $[\text{Fe}/\text{H}]_{\text{J95}} = 1.431[\text{Fe}/\text{H}]_{\text{ZW84}} + 0.880$ (Jurcsik 1995). This gives a mean metallicity for the RRab stars of $[\text{Fe}/\text{H}]_{\text{ZW84}} = -1.65 \pm 0.10$. This is more metal-rich than the literature values, though it is con-

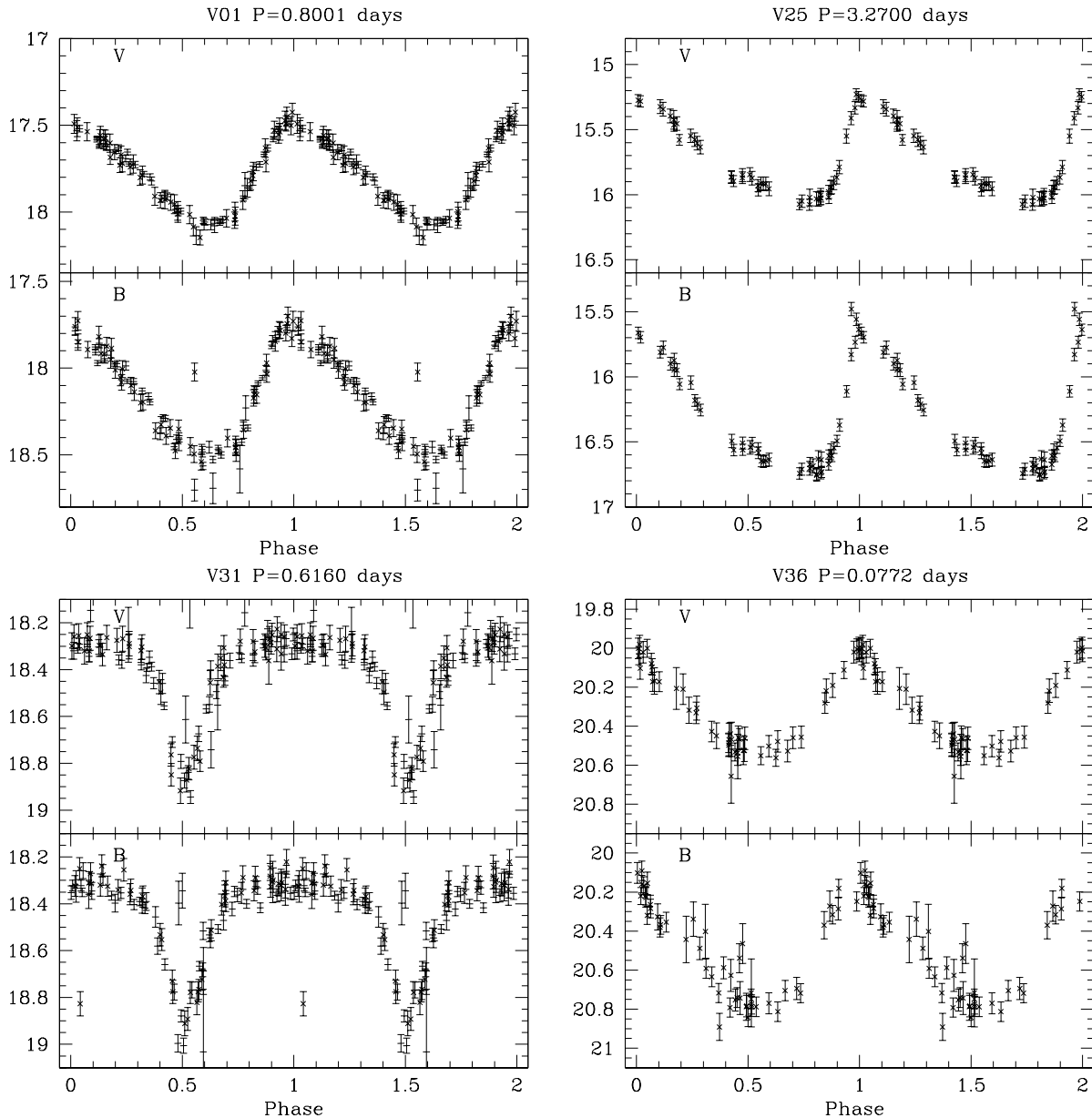


Figure 8. Sample light curves for the non-RR Lyrae variable stars in NGC 1786. V01 is an Anomalous Cepheid while V25 is a classical Cepheid. The second row shows the light curves of one of the eclipsing binaries and one of the Delta Scuti/SX Phoenicis stars. SOAR data is indicated with crosses while SMARTS data is indicated by points with horizontal lines. (The full set of light curves can be found in the electronic version of this paper.)

sistent within the error bars. If we consider only the two stars with the smallest D_{max} (V08 and V10), indicating that they have the most regular light curves, the average metallicity becomes $[\text{Fe}/\text{H}]_{\text{ZW84}} = -1.96 \pm 0.13$. This value is more metal poor than the literature values. The mean metallicity found for the RRc stars is $[\text{Fe}/\text{H}]_{\text{ZW84}} = -1.92 \pm 0.06$, which is more metal-poor than any of the literature values but is consistent with the value for the two RRab stars with the lowest D_{max} values. The LMC field RRc star, V35, in Table 8 immediately stands out by being much more metal-rich than any of the other RRc stars. In the new UVES scale (Carretta et al. 2009) these metallicities are $[\text{Fe}/\text{H}]_{\text{UVES}} = -2.04 \pm 0.19$ for the two RRab stars with

the lowest D_{max} values and $[\text{Fe}/\text{H}]_{\text{UVES}} = -1.99 \pm 0.10$.

5. DISTANCE MODULUS

The absolute magnitude-metallicity relationship from Catelan & Cortés (2008) is used to find the absolute magnitude of the RR Lyrae stars in NGC 1786. Since the metallicity obtained for the RRab stars, $[\text{Fe}/\text{H}]_{\text{ZW84}} = -1.65 \pm 0.10$, is closer to the metallicities reported in the literature, it is used for this calculation, giving a V absolute magnitude of $\langle M_V \rangle = 0.60 \pm 0.22$. Using the mean observed V magnitude for the RRab stars, $\langle V \rangle = 19.176 \pm 0.085$, the reddening value given by Sharma et al. (2010), $E(B-V) = 0.06$, and a standard extinction law with $A_V/E(B-V) = 3.1$ gives a reddening-corrected distance modulus of $(m - M)_0 =$

Table 6
Fourier Coefficients for RRc Variables

ID	A_1	A_{21}	A_{31}	A_{41}	ϕ_{21}	ϕ_{31}	ϕ_{41}	Order
V07	0.274	0.284	0.121	0.079	4.44	2.23±0.36	1.22	8
V11	0.276	0.202	0.109	0.051	4.70	2.67±0.43	1.58	6
V37	0.231	0.109	0.073	0.026	4.40	2.35±0.82	5.90	6
V44	0.246	0.171	0.088	0.054	4.93	3.66±0.43	3.02	8
V45	0.285	0.303	0.103	0.060	3.94	2.17±1.11	1.15	8
V62	0.128	0.223	0.122	0.042	3.49	2.19±0.50	1.11	7
V35-Field	0.242	0.066	0.062	0.035	5.31	4.17±0.46	2.64	7

Table 7
Derived Physical Properties for RRab Variables

ID	[Fe/H] _{J95}	$\langle M_V \rangle$	$\langle V - K \rangle$	$\log T_{\text{eff}}^{(V-K)}$	$\langle B - V \rangle$	$\log T_{\text{eff}}^{(B-V)}$	$\langle V - I \rangle$	$\log T_{\text{eff}}^{(V-I)}$
V03	-1.625	0.695	1.166	3.805	0.332	3.811	0.486	3.812
V04	-1.399	0.737	1.073	3.814	0.301	3.824	0.446	3.822
V05	-1.346	0.709	1.247	3.795	0.380	3.797	0.546	3.796
V08	-1.741	0.764	1.184	3.803	0.347	3.807	0.503	3.808
V10	-2.106	0.649	1.342	3.787	0.377	3.793	0.5431	3.798
V26	-1.120	0.711	1.232	3.796	0.388	3.795	0.557	3.793
V38	-0.994	0.708	1.223	3.796	0.396	3.794	0.566	3.790
Mean	-1.476±0.144	0.710±0.134	1.210±0.031	3.800±0.001	0.3602±0.013	3.803±0.004	0.521±0.017	3.803±0.004

18.39 ± 0.24. This agrees with the distance modulus of $(m - M)_{LMC} = 18.44 \pm 0.11$ that Catelan & Cortés (2008) derived for the LMC. The location of NGC 1786 is near the center of the LMC, and the cluster distance modulus is expected to be similar to that of the LMC.

We can also use the Type II Cepheid, V41, and the Anomalous Cepheid, V01, to check the distance modulus. Using the period-luminosity relationships for Type II Cepheids from Pritzl et al. (2003) we obtain absolute magnitudes of $\langle M_V \rangle = -0.02 \pm 0.09$ and $\langle M_B \rangle = 0.26 \pm 0.14$ for V41. Using the same values for reddening as we used for the RR Lyrae stars, this gives us a reddening-corrected distance modulus of $(m - M)_0 = 18.37 \pm 0.17$ which is consistent with what was obtained for the RR Lyrae stars.

V01 displays a shape that suggests that it is an Anomalous Cepheid which pulsates in the first overtone. Using the period-amplitude relationships for first overtone ACs from Pritzl et al. (2002), we obtain absolute V and B magnitudes of $\langle M_V \rangle = -1.25 \pm 0.09$ and $\langle M_B \rangle = -1.04 \pm 0.12$. This leads to a reddening-corrected distance modulus of $(m - M)_0 = 18.88 \pm 0.16$, which is longer than any of the other values. If we instead assume that V01 is pulsating in the fundamental mode, we then obtain absolute V and B magnitudes of $m - M_V = -0.45 \pm 0.05$ and $m - M_B = -0.15 \pm 0.06$ which yield a reddening-corrected distance modulus of $(m - M)_0 = 18.04 \pm 0.08$, which is shorter than any of the other values.

6. OOSTERHOFF CLASSIFICATION

The average periods for the RR Lyrae stars in NGC 1786 are $\langle P_{ab} \rangle = 0.608$ days and $\langle P_c \rangle = 0.336$ days. The division between Oosterhoff-intermediate and Oo-II clusters occurs at an average RRab period of 0.62 days; the average RRab period for NGC 1786 is just on the Oo-int side of this division. Traditionally the average RRc period has also been used as an indicator of Oosterhoff status, and an average period of 0.335 days would

suggest an Oo-I classification for NGC 1786. However, Catelan et al. (2012) recently found that average RRc period is not a strong indicator of Oosterhoff status due to the overlap in $\langle P_c \rangle$ values between clusters of all three Oosterhoff types; in fact an average RRc period of 0.336 days would be consistent with any Oosterhoff classification.

We found 26 RRab, 17 RRc, and 8 RRd stars within the tidal radius of NGC 1786 which gives the cluster a $N_{c+d}/N_{c+d+ab} = 0.49$. This ratio of first overtone pulsators to total number of RR Lyrae stars suggests an Oo-II classification for the cluster; though it would be similar to the highest ratio seen in Oo-int clusters. The minimum RRab period in the cluster is $P_{ab,min} = 0.49336$ days, which suggests an Oo-Int classification.

Figure 9 shows the V - and B -band period-amplitude diagrams for NGC 1786. Both diagrams show a great deal of scatter in the location of both the RRab and RRc stars. The scatter in the RRab stars appears to rise from two reasons. The three RRab's in the central region of the cluster, denoted as squares, all have amplitudes that are small for their period. An examination of their light curves shows that all three contain messy light curves that show signs of possible blending, which is not surprising considering that they are located toward the center of a crowded cluster. Additionally, V50 has few data points near maximum light, and thus its amplitude, computed by template fitting, may be too low due to its missing maximum light in our data. The 5 RRab stars that were previously mentioned as being more than one magnitude too bright and showing clear evidence of blending are not included in these figures.

Looking at the RRab stars that are between 21 and 55 arcseconds from the cluster center (indicated with blue plus signs), one sees very little scatter with all the stars located near the Oo-II locus. This region potentially provides the best representation of the RR Lyrae stars in the

Table 8
Derived Physical Properties for RRc Variables

ID	[Fe/H] _{ZW84}	$\langle M_V \rangle$	M/M_\odot	$\log(L/L_\odot)$	$\log T_{\text{eff}}$	Y
V07	-1.804	0.685	0.739	1.730	3.864	0.261
V11	-1.819	0.689	0.685	1.734	3.862	0.263
V37	-2.112	0.700	0.790	1.806	3.853	0.240
V44	-1.820	0.634	0.575	1.742	3.859	0.266
V45	-1.850	0.725	0.755	1.738	3.863	0.259
V62	-2.139	0.733	0.833	1.827	3.851	0.234
V35-Field	-1.197	0.672	0.480	1.668	3.868	0.292
Mean	-1.924 ± 0.064	0.694 ± 0.014	0.699 ± 0.047	1.763 ± 0.017	3.859 ± 0.002	0.259 ± 0.007

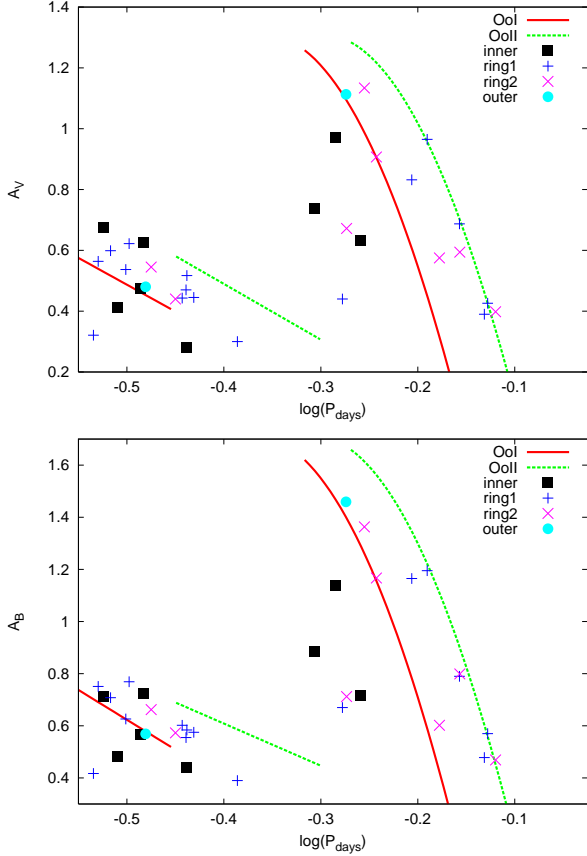


Figure 9. Bailey diagram, log period vs V -band (top panel) or B -band (bottom panel) amplitude for the RR Lyrae stars in NGC 1786. Red and green lines indicate the typical position for RR Lyrae stars in Oosterhoff I and Oosterhoff II clusters, respectively (Cacciari et al. 2005; Zorotovic et al. 2010). Black squares indicate stars within 21 arcseconds of the cluster center, blue plus signs indicate stars between 21 and 55 arcseconds from the center, magenta \times ’s indicate stars farther than 55 arcseconds but still within the tidal radius of NGC 1786, while blue circles indicate stars outside of the tidal radius.

cluster as it is far enough from the center of the cluster that the stars should not be impacted by blending but are still likely to be cluster members. Magenta \times symbols show the RR Lyrae stars that are farther than 55 arcseconds from the cluster center but still within the tidal radius. The RRab stars in this region show more scatter, which could be due to a greater chance of some of them being LMC field stars. Blue circles indicate the stars that are outside of the tidal radius.

The RRc stars tend to be located closer to the Oo-I

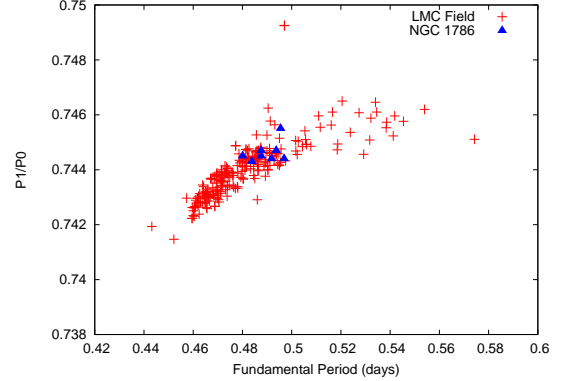


Figure 10. Petersen diagram showing the ratio of the first overtone period to the fundamental-mode period vs. fundamental-mode period for the RRd stars in NGC 1786 (blue triangles). Also plotted are the RRd stars in the LMC field (red plus symbols) from Soszyński et al. (2003).

locus, which would be consistent with the average RRc periods being more similar to what is seen in Oo-I clusters. There does not seem to be any major shift in the position of the RRc stars with distance from the cluster center.

Figure 10 shows the Petersen diagram which includes the RRd stars in NGC 1786 as well as those in the LMC field. The RRd stars in NGC 1786 fall in the same region as RRd stars in Milky Way Oo-I objects, that is, in the shorter period range ($\approx 0.48 - 0.50$ days), while Oo-II RRd generally have longer periods ($\approx 0.53 - 0.55$ days; see, e.g., Fig. 1 in Popielski et al. (2000), and Fig. 13 in Clementini et al. (2004)).

The contamination from LMC field RR Lyrae impacts the Oosterhoff classification of the cluster and without radial velocities to determine definitive cluster membership of the RR Lyrae stars it is difficult to come up with a definitive classification. However, we can get a better handle on the Oosterhoff classification using the previously mentioned comparison field from the OGLE-III data which found 7 RRab and 2 RRc stars in an annulus with an area equal in size to the area within the tidal radius of NGC 1786. Since the vast majority of the RR Lyrae stars in this comparison field were RRab stars, it is reasonable to expect that the majority of the field stars within the tidal radius are also RRab stars. This would mean the actual value of N_{c+d}/N_{c+d+ab} would be higher than the value we obtained which would be more consistent with an Oo-II classification. Figure 11 shows the V -band period-amplitude diagram for the comparison field. The majority of the RRab stars fall near the Oo-I locus. Combining this with the fact that Figure 9 shows that

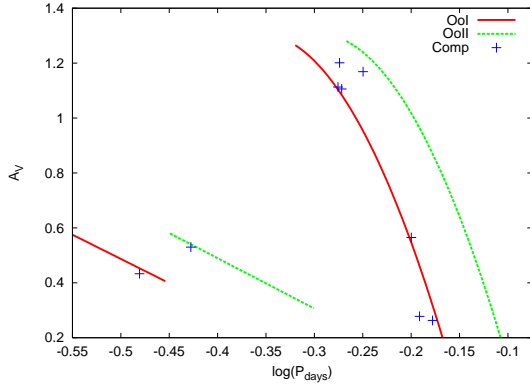


Figure 11. V-band Bailey diagram for the RR Lyrae stars in the control field from the OGLE-III data Soszyński et al. (2009). The control field is an annulus centered on NGC 1786 with the same area on the sky as the area in the tidal radius of the cluster. The red and green lines indicate the typical position for RR Lyrae stars in Oosterhoff I and Oosterhoff II clusters, respectively (Cacciari et al. 2005; Zorotovic et al. 2010).

the RRab stars near the Oo-I locus are located further from the cluster center it is reasonable to conclude that these RRab are likely to be LMC field stars and the majority of the non-blended RRab stars that are actually members of NGC 1786 are located near the Oo-II locus.

The Oosterhoff classification of NGC 1786 is more complicated than that of the other clusters examined in this study. The first overtone dominant pulsators, the RRC and RRd stars, display properties similar to what is seen in Oo-I clusters. However, the fundamental-mode pulsators, the RRab stars, suggest an Oo-Int classification. The picture is further complicated by the fact that some of the RR Lyrae within the tidal radius are likely LMC field stars and should not be included when looking at the behavior of the cluster RR Lyrae stars. The Oo-Int-like behavior of the RRab stars may be a result of this contamination.

7. CONCLUSIONS

We conducted a photometric study of NGC 1786 in order to identify and classify variable stars within the cluster. A total of 65 variable stars were found in our field of view, 53 of which were RR Lyrae stars (27 RRab, 18 RRC, and 8 RRd). 4 of the variable stars (1 RRab, 1 RRC, 1 classical Cepheid, and 1 Delta Scuti/SX Phoenicis) were outside the tidal radius of the cluster and thus are likely to be LMC field stars. The location of NGC 1786 near the center of the LMC means that field contamination is likely within the tidal radius, however, we expect most of the variable stars found within NGC 1786’s tidal radius to be cluster members.

We obtained Fourier parameters for some of the RR Lyrae stars and used these parameters to calculate physical properties of these stars. The calculated physical properties will be compared to properties for RR Lyrae stars in other clusters in a future paper in this series. We obtained a reddening-corrected distance modulus of $(m - M)_0 = 18.48 \pm 0.23$ from the six RRab stars which did not have any nearby neighbors which could cause issues with blending.

The average RRab period of NGC 1786 suggests an Oo-int classification for the cluster, though it is near the division between Oo-int and Oo-II, while the number ratio of first overtone dominant pulsators to total number of

RR Lyrae stars suggests an Oo-II classification. There is a great deal of scatter amongst the RRab stars on the Bailey diagram that is likely due to contamination from the LMC field stars; a comparison field suggests that the RRab stars that are cluster members likely appear more like those seen in Oo-II clusters. The behavior of the RRC stars on the Bailey diagram and the RRd stars on the Petersen diagram both are more consistent with an Oo-I classification, while the average RRC period is consistent with either any of the three Oosterhoff types. The behavior of the RR Lyrae on the Bailey diagram and how it compares to what is seen in other clusters will be discussed in more detail in a future paper in this series. Physical properties for some of the RR Lyrae were obtained via Fourier decomposition of the light curves and these properties will be compared to the properties determined for the other clusters in this study in a future paper.

Support for H.A.S. and C.A.K. is provided by NSF grants AST 0607249 and AST 0707756. M.C. is supported by Proyecto Fondecyt Regular #1110326; BASAL Center for Astrophysics and Associated Technologies (PFB-06); the Chilean Ministry for the Economy, Development, and Tourism’s Programa Iniciativa Científica Milenio through grant P07-021-F, awarded to The Milky Way Millennium Nucleus; and Proyecto Anillo ACT-86. JB is supported by the Chilean Ministry for the Economy, Development, and Tourism’s Programa Iniciativa Científica Milenio through grant P07-02-F, awarded to The Milky Way Millennium Nucleus and FONDECYT regular No. 1120601.

REFERENCES

- Alard, C. 2000, *A&AS*, 144, 363
 Bica, E., Bonatto, C., Dutra, C.M., & Santos, J.F.C. 2008, *MNRAS*, 389, 678
 Cacciari, C., Corwin, T. M., & Carney, B.W. 2005, *AJ*, 129, 267
 Carretta, E. et al. 2009, *A&A*, 508, 695
 Catelan, M. 2009, *Ap&SS*, 320, 261
 Catelan, M., & Cortés, C. 2008, *ApJ*, 676, L135
 Catelan, M., et al. 2012, *AJ*, submitted
 Clementini, G., Corwin, T. M., Carney, B. W., & Sumerel, A. N. 2004, *AJ*, 127, 938
 Graham, J.A. 1985, *PASP*, 97, 676
 Johnson, J.A., Bolte, M., Stetson, P.B., & Hesser, J.E. 2002, *IAU Symp.* 207, 190
 Jurcsik, J. 1995, *AcA*, 45, 653
 Jurcsik, J. 1998, *A&A*, 333, 571
 Jurcsik, J., & Kovács, G. 1996, *A&A*, 312, 111
 Kovács, G., & Walker, A.R. 1999, *ApJ*, 512, 271
 Kovács, G., & Walker, A.R. 2001, *A&A*, 371, 579
 Kuehn, C.A. et al. 2011, *AJ*, 142, 107
 McLaughlin, D.E., & van der Marel, R.P. 2005, *ApJS*, 161, 304
 Morgan, S.M., Wahl, J.N., & Wiekhorst, R.M. 2007, *MNRAS*, 374, 1421
 Mucciarelli, A., Origlia, L., Ferraro, F. R., & Pancino, E. 2009, *ApJ*, 695, 134
 Olszewski, E.W., Schommer, R.A., Suntzeff, N.B., & Harris, H.C. 1991, *AJ*, 101, 515
 Popielski, B. L., Dziembowski, W. A., & Cassisi, S. 2000, *AcA*, 50, 491
 Pritzl, B.J., Armandroff, T.E., Jacoby, G.H., & Da Costa, G.S. 2002, *AJ*, 124, 1464
 Pritzl, B.J. et al. 2003, *AJ*, 126, 1381
 Sharma, S., Borissova, J., Kurtev, R., Ivanov, V.D., & Geisler, D. 2010, *AJ*, 139, 878
 Simon, N.R., & Clement, C.M. 1993, *ApJ*, 410, 526

Soszyński, I., et al. 2003, *AcA*, 53, 93

Soszyński, I., et al. 2009, *AcA*, 59, 1

Stetson, P.B. 2000, *PASP*, 112, 925

Udalski, A., Szymanski, M.K., Soszynski, I., & Poleski, R. 2008,
AcA, 58, 69

Walker, A.R. & Mack, P. 1988, *AJ*, 96, 1362

Zinn, R., & West, M.J. 1984, *ApJS*, 55, 45

Zorotovic, M., et al. 2010, *AJ*, 139, 357; erratum: 2010, *AJ*, 140,
912